Electronic Supplementary Material (ESI) for Dalton Transactions.

Supporting Information for

"The unusual metal ion binding ability of histidyl tags and their mutated derivatives"

Davide Brasili,[a] Joanna Watly, [b] Eyal Simonovsky, [cd] Remo Guerrini,[a] Nuno A. Barbosa, [b]

Robert Wieczorek[b], Maurizio Remelli[a], Henryk Kozlowski[b*] and Yifat Miller[cd*]

[a] *Department of Chemical and Pharmaceutical Sciences, University of Ferrara, via Fossato di Mortara 17, I-44121 Ferrara, Italy. E-mail: rmm@unife.it*

[b] *Department of Chemistry, University of Wroclaw, F. Joliot-Curie 14, 50-383 Wroclaw, Poland. E-mail: henryk.kozlowski@chem.uni.wroc.pl*

[c] *Department of Chemistry and* [d]*Ilse Katz Institute for Nanoscale Science and Technology, Ben Gurion University of the Negev, Beer-Sheva 84105, Israel. E-mail: ymiller@bgu.ac.il*

Table S1: Complex-formation constants for the ligand L1 with Cu(II), at T = 298 °K and I = 0.1 mol·dm^{-3} (KCl). Standard deviations on the last figure in parentheses.

Species	**Log β**	**pK_a**
$[CuLH_3]^{2+}$	25.68 (6)	4.3
$[CuLH_2]^{+}$	21.38 (3)	5.19
[CuLH]	16.19 (4)	6.82
$[CuL]^{-}$	9.37 (6)	7.87
$[CuLH_{-1}]^{2-}$	1.50 (7)	8.25
$[CuLH_{-2}]^{3-}$	-6.75 (8)	10.05
$[CuLH_{-3}]^{4-}$	-16.8 (1)	-

Table S2: Complex-formation constants for the ligand L2 with Cu(II), at T = 298 °K and I = 0.1 mol·dm^{-3} (KCl). Standard deviations on the last figure in parentheses.

Species	Log β	pK_a
$[CuLH_4]^{3+}$	32.26 (5)	4.44
$[CuLH_3]^{2+}$	27.82 (4)	4.58
$[CuLH_2]^{+}$	23.24 (3)	5.91
[CuLH]	17.33 (4)	6.43
$[CuL]^{-}$	10.90 (5)	-
$[CuLH_{-2}]^{3-}$	-5.16 (6)	9.40
$[CuLH_{-3}]^{4-}$	-14.56 (8)	-

Table S3: Spectroscopic parameters at different pH values for the system Cu(II)/L1; $C°_{Cu(II)} = 5 \cdot 10^{-4}$ mol·dm^{-3}; M/L ratio = 1.1.1.

		UV-Vis		CD		EPR	
pH	**Species**	**λ/nm**	**ε/M^{-1}cm^{-1}**	**λ/nm**	**$\Delta\varepsilon$/M^{-1} cm^{-1}**	**A_{II} (G)**	**g_{II}**
4.5	$[CuLH_3]^{2+}$ $[CuLH_2]^{+}$	663	41.1	254	0.15	164	2.32
5.0	$[CuLH_2]^{+}$ $[CuLH]$	635	67.2	580 250	-0.13 1.36	166	2.28
5.6	$[CuLH_2]^{+}$ $[CuLH]$	622	80.8	586 252	-0.21 2.17		
6.2	[CuLH] $[CuL]^{-}$	610	87.7	570 245	-0.25 2.89	173	2.27
7.1	$[CuL]^{-}$ [CuLH] $[CuLH_{-1}]^{2-}$	608	90	570 250 677	-0.25 3.11 0.10	186	2.25
7.5	$[CuL]^{-}$ [CuLH] $[CuLH_{-1}]^{2-}$	603	92	557 457 341 250	-0.30 0.06 -0.13 3.47		
8.0	$[CuL]^{-}$ $[CuLH_{-1}]^{2-}$ $[CuLH_{-2}]^{3-}$	596	106	640 548 478 336 250	0.21 -0.44 0.99 -1.07 4.77	188	2.23
8.6	$[CuLH_{-1}]^{2-}$ $[CuLH_{-2}]^{3-}$	577	123	633 551 474 335 252	0.44 -0.46 0.16 -1.72 5.41		
9.1	$[CuLH_{-1}]^{2-}$ $[CuLH_{-2}]^{3-}$	562	140	638 551 474 335 254	0.51 -0.46 0.16 -1.72 5.59	188	2.23
9.6	$[CuLH_{-2}]^{3-}$ $[CuLH_{-3}]^{4-}$	558	130	635 531 402 337 254	0.80 -0.26 0.16 -1.24 5.96		
10.3	$[CuLH_{-2}]^{3-}$ $[CuLH_{-3}]^{4-}$	530	128	631 487 402 345 260	0.96 -0.70 0.06 -0.53 6.12	186	2.22
11.2	$[CuLH_{-3}]^{4-}$	521	135	626 486 402 318 294 258	1.37 -1.18 0.02 0.76 -0.19 6.78	193	2.19

Table S4: Spectroscopic parameters at different pH values for the system Cu(II)/L2; $C°_{Cu(II)} = 5 \cdot 10^{-4}$ mol·dm^{-3}; M/L ratio = 1.1.1.

		UV-Vis		CD		EPR	
pH	**Species**	**λ/nm**	**ε/M^{-1}cm^{-1}**	**λ/nm**	**$\Delta\varepsilon$/M^{-1} cm^{-1}**	**A_{II} (G)**	**g_{II}**
4.7	$[CuLH_4]^{3+}$ $[CuLH_3]^{2+}$ $[CuLH_2]^{+}$	659	36.1	252	0.63	164	2.31
5.2	$[CuLH_3]^{2+}$ $[CuLH_2]^{+}$	639	52.0	249	1.30	169	2.28
6.2	$[CuLH_2]^{+}$ [CuLH] $[CuL]^{-}$	607	68.1	246	1.75	-	-
6.7	[CuLH] $[CuL]^{-}$	607	69.3	246	2.00	173	2.27
7.2	$[CuL]^{-}$	602	73.4	247	2.44		
7.7	$[CuL]^{-}$ $[CuLH_{-2}]^{3-}$	588	82.6	635 557 251	0.07 -0.19 2.75	182	2.25
8.4	$[CuL]^{-}$ $[CuLH_{-2}]^{3-}$	579	89.8	636 549 476 335 247	0.20 -0.39 0.09 -1.21 4.41	186	2.21
8.8	$[CuLH_{-2}]^{3-}$ $[CuLH_{-3}]^{4-}$	556	100.6	632 548 402 336 249	0.40 -0.58 0.02 -1.76 5.91	-	-
10.0	$[CuLH_{-2}]^{3-}$ $[CuLH_{-3}]^{4-}$	537	105.06	624 517 404 339 256	0.83 -0.42 0.10 -0.96 6.37	188	2.20
10.9	$[CuLH_{-3}]^{4-}$	522	108.5	624 485 353 316 294 259	1.18 -0.99 -0.24 0.70 0.25 6.46	191	2.20
11.5	$[CuLH_{-3}]^{4-}$	518	109.3	626 489 358 320 294 261	1.24 -1.13 -0.16 0.87 -0.16 6.84	-	-

Table S5: Metal-ligand interactions (L1a and L1b complexes).

X	Cu-X [Å]
	L1a
His7	1.832
His11	1.835
	L1b
His5	2.440
His7	1.849
His11	1.841

Table S6: Metal-ligand interactions (L2 complex).

X	Cu-X [Å]
	L2
His4	1.875
His6	2.130
His10	1.901

Table S7: Hydrogen bonds of L1a and L1b complexes. Fragments marked with star supply hydrogen bond with atoms form side chains.

Residue	H..PA [Å]	PD-H..PA [deg]	Fragment	HB type
		L1a		
D2..H11	1.604	162.3	C=O*..H-N*	
D2..H11	1.637	170.6	C=O*..H-N	
A6..A8	2.195	157.8	N-H..O=C	3-10 helix
A6..H9	2.105	151.3	C=O..H-N*	
Ac..D2	2.005	153.8	C=O(Ac)..H-N	
Ac..D2	1.828	168.4	C=O(Ac)..H-N	
		L1b		
H5...A12	1.878	166.2	N-H*..O=C	
E1..H11	1.703	163.0	N-H..O=C*	
H7..H9	2.461	162.7	C=O..H-N	3-10 helix
A6..A8	1.905	167.1	C=O..H-N	3-10 helix
D2..D3	1.950	168.6	C=O*..H-N	
Ac..A6	1.847	162.5	C=O(Ac)..H-N	

Table S8: Hydrogen bonds of S2 complex. Fragments marked with star supply hydrogen bond with atoms form side chains.

Residue	H..PA [Å]	PD-H..PA [deg]	Fragment	HB type
		S2		
E1..D3	1.987	150.7	N-H..O=C*	
D3..H4	1.180	153.6	C=O*..H-N*	
D3..A5	1.679	167.9	O=C..N-H	3-10 helix
H4..H6	2.001	165.6	O=C..N-H	3-10 helix
A5..A7	1.788	165.0	O=C..N-H	3-10 helix
H6..H8	2.181	164.9	O=C..N-H	3-10 helix
A7..A9	2.095	156.2	O=C..N-H	3-10 helix
A7..NH_2	2.079	158.8	O=C..N-H_2	
H4..G13	1.704	162.3	N-H*..O=C	
H10..A11	1.670	154.2	N-H..O=C	

Table S9: Conformational energies and populations obtained from the GBMV and Monte-Carlo calculations.

Peptide	Averaged conformational energy [kcal/mol]	Standard error of the averaged conformational energy values [kcal/mol]	Populations (%)
L1a	-819.9	0.7	27
L1b	-861.0	0.6	73

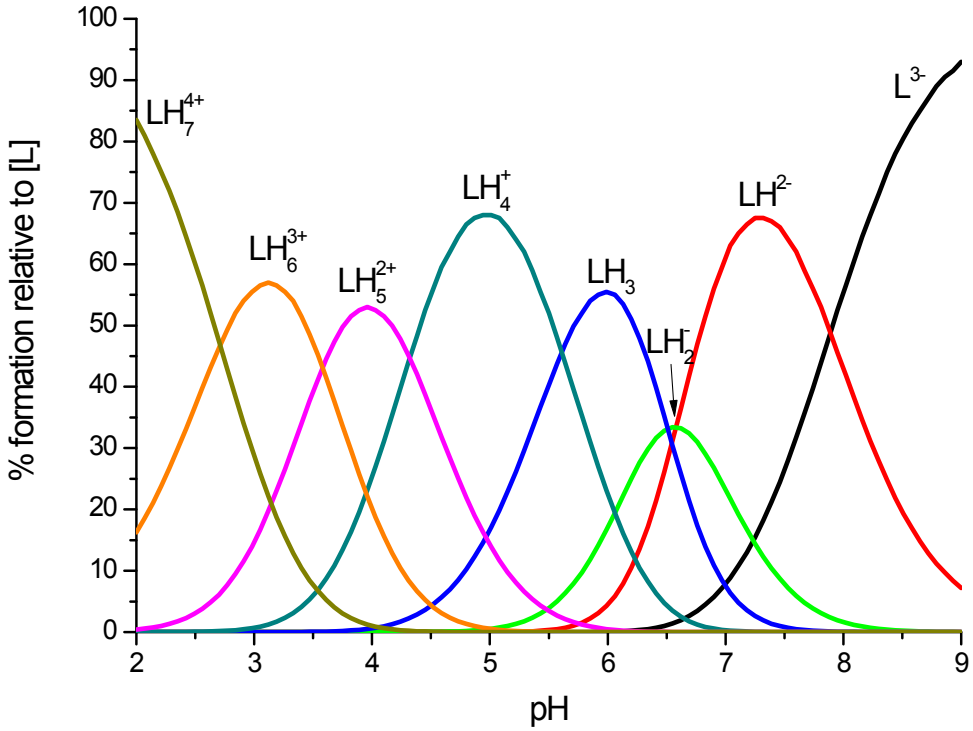

Figure S1. Species distribution diagram for the protonation equilibria of the ligand L1; $C°_L = 6 \cdot 10^{-4}$ mol·dm^{-3}.

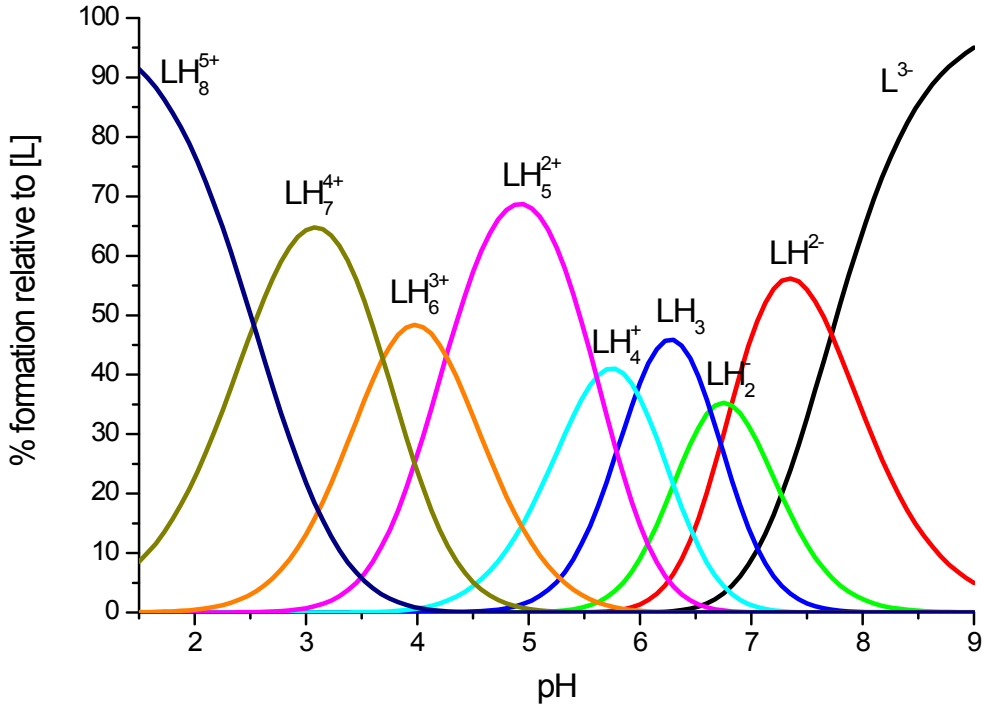

Figure S2. Species distribution diagram for the protonation equilibria of the ligand L2; $C°_L = 6 \cdot 10^{-4}$ mol·dm^{-3}.

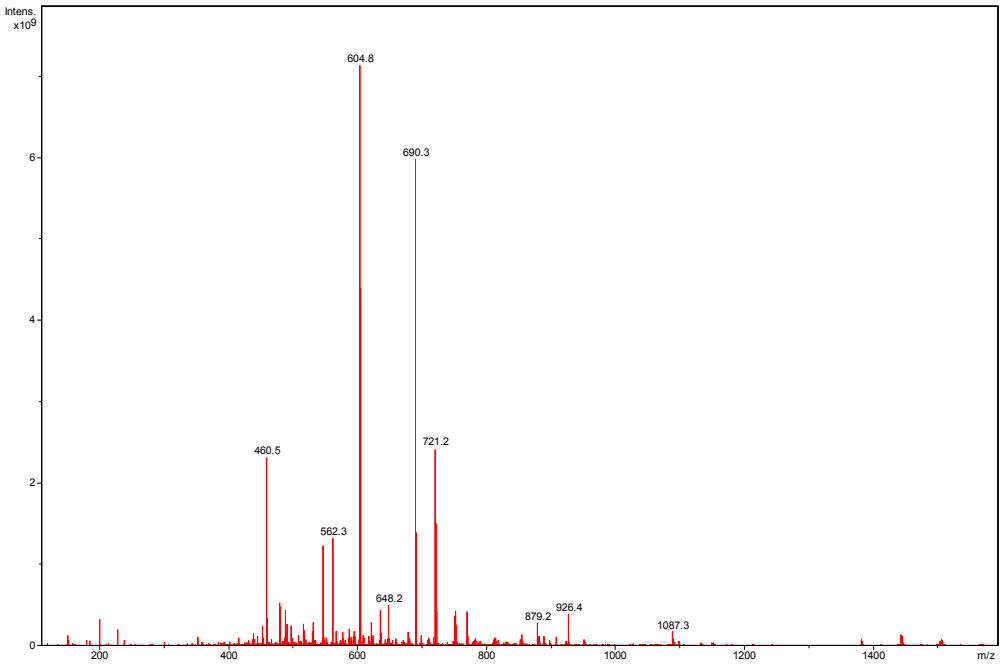

Figure S3. ESI-MS spectrum of the system Cu(II)/L1; $C°_{Cu(II)} = 5 \cdot 10^{-4}$ mol·dm^{-3}; M/L ratio = 2.1; pH = 5; positive ion mode.

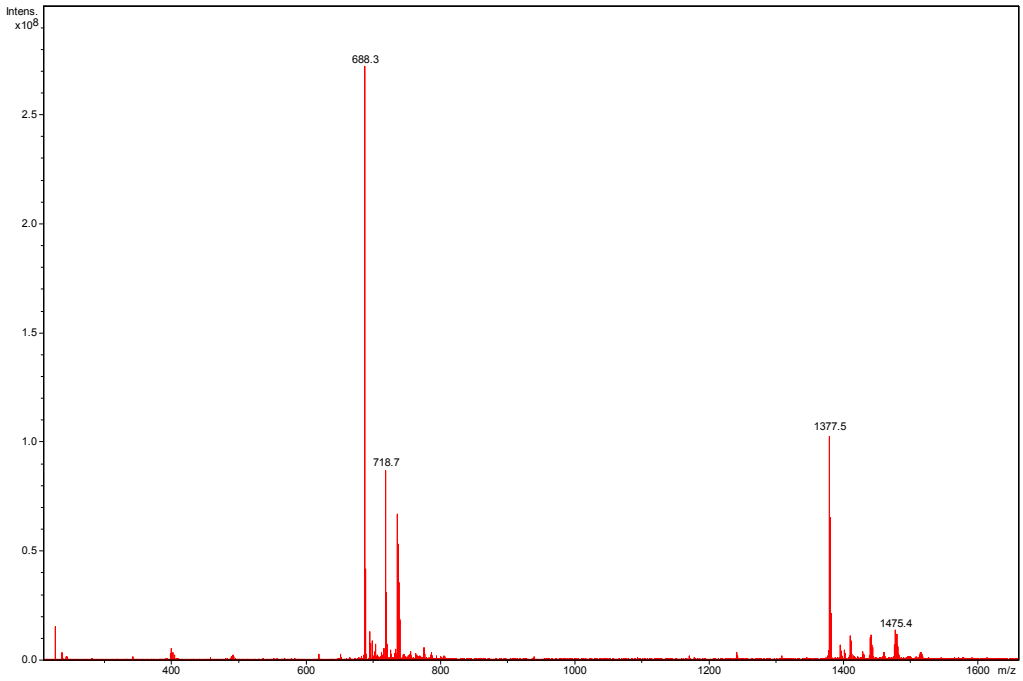

Figure S4 ESI-MS spectrum of the system Cu(II)/L1; $C°_{Cu(II)} = 5 \cdot 10^{-4}$ mol·dm^{-3}; M/L ratio = 2.1; pH = 5; negative ion mode.

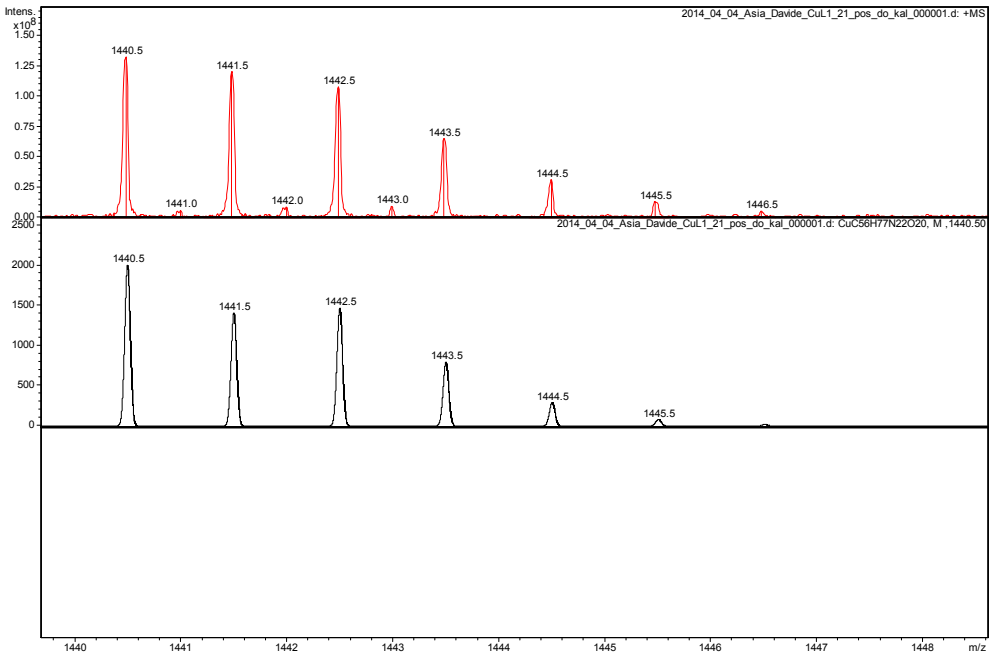

Figure S5. Experimental (up) and simulated (down) ESI-MS spectrum for the complex $[CuLH_2]^+$ ($CuC_{56}H_{77}N_{22}O_{20}$, MW = 1440.6) in the system Cu(II)/L1; $C°_{Cu(II)} = 5 \cdot 10^{-4}$ mol·dm^{-3}; M/L ratio = 2.1; pH = 5; positive ion mode.

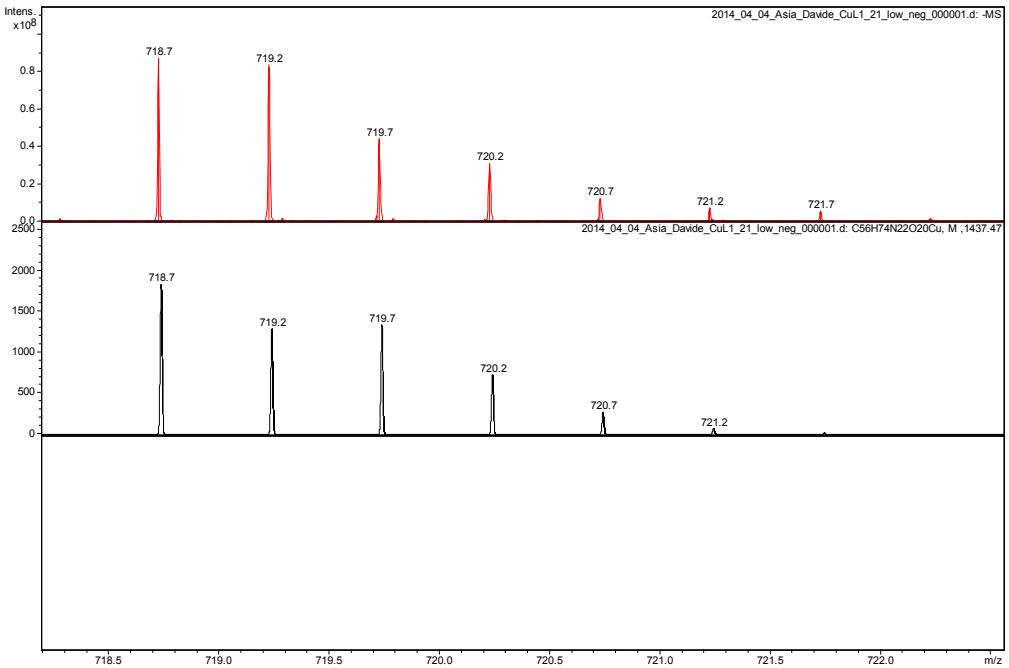

Figure S6. Experimental (up) and simulated (down) ESI-MS spectrum for the complex $[CuLH_{-1}]^{2-}$ ($CuC_{56}H_{74}N_{22}O_{20}$, MW = 1437.6) in the system Cu(II)/L1; $C°_{Cu(II)} = 5 \cdot 10^{-4}$ mol·dm^{-3}; M/L ratio = 2.1; pH = 5; negative ion mode.

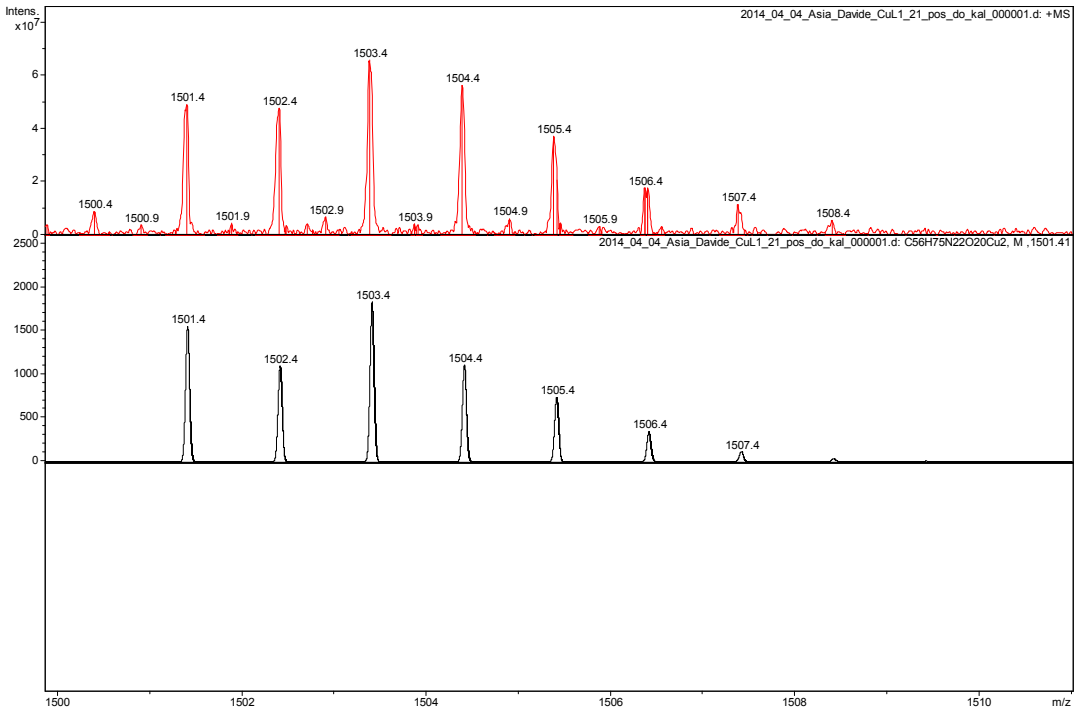

Figure S7. Experimental (up) and simulated (down) ESI-MS spectrum for the complex $[Cu_2L]^+$ ($Cu_2C_{56}H_{75}N_{22}O_{20}$, MW = 1501.4) in the system Cu(II)/L1; $C°_{Cu(II)} = 5 \cdot 10^{-4}$ mol·dm^{-3}; M/L ratio = 2.1; pH = 5; positive ion mode.

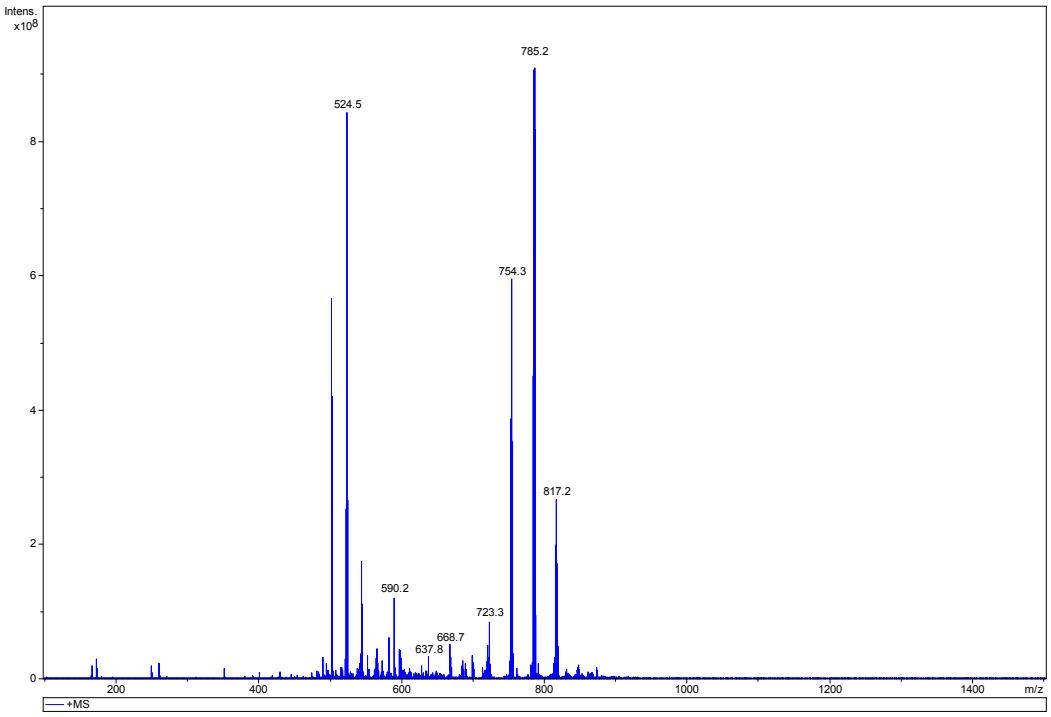

Figure S8. ESI-MS spectrum of the system Cu(II)/L2; $C°_{Cu(II)} = 5 \cdot 10^{-4}$ mol·dm^{-3}; M/L ratio = 2.1; pH = 5; positive ion mode.

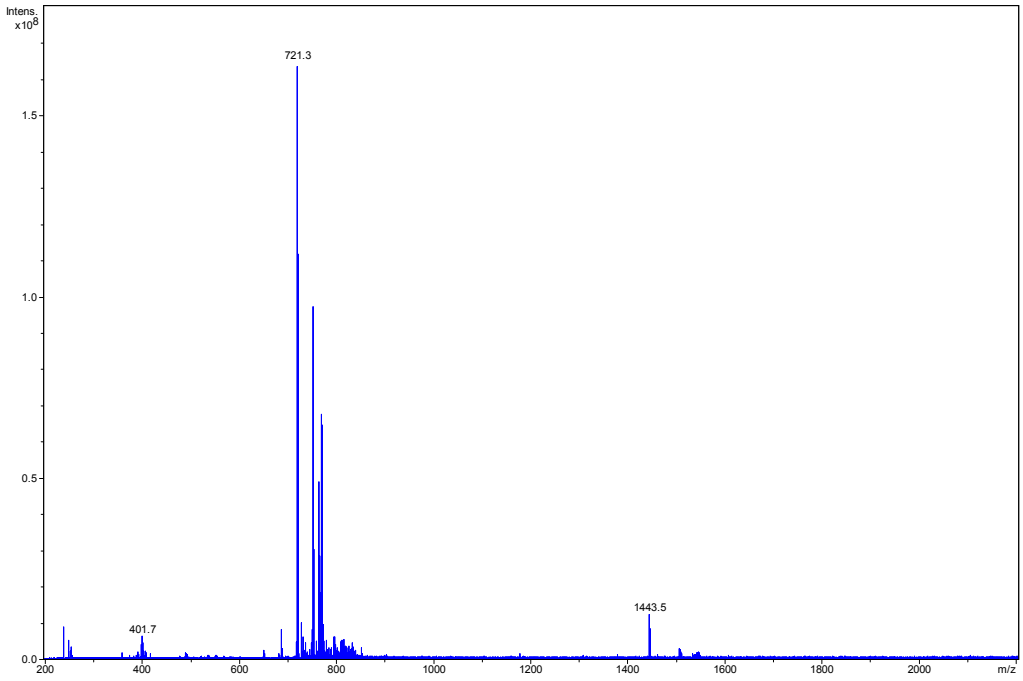

Figure S9. ESI-MS spectrum of the system Cu(II)/L2; $C°_{Cu(II)} = 5 \cdot 10^{-4}$ mol·dm^{-3}; M/L ratio = 2.1; pH = 5; negative ion mode.

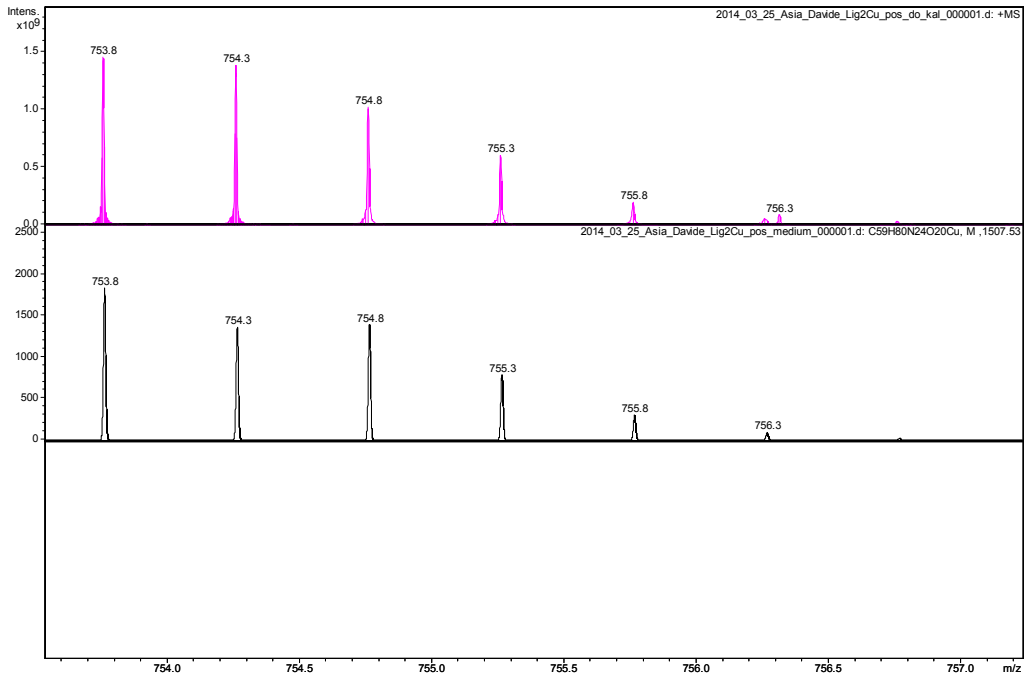

Figure S10. Experimental (up) and simulated (down) ESI-MS spectrum for the complex $[CuLH_3]^{2+}$ ($CuC_{59}H_{80}N_{24}O_{20}$, MW = 1507.6) in the system Cu(II)/L2; $C°_{Cu(II)} = 5 \cdot 10^{-4}$ mol·dm^{-3}; M/L ratio = 2.1; pH = 5; positive ion mode.

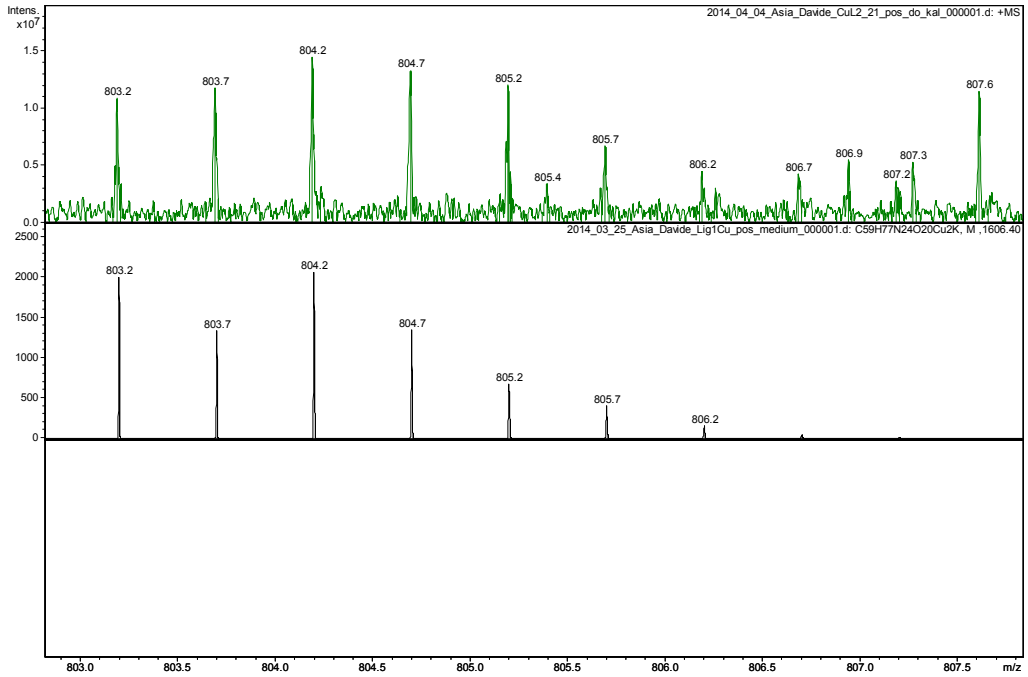

Figure S11. Experimental (up) and simulated (down) ESI-MS spectrum for the complex $[Cu_2L]K^{2+}$ ($Cu_2C_{59}H_{77}N_{24}O_{20}K$, MW = 1606.4) in the system Cu(II)/L2; $C°_{Cu(II)} = 5 \cdot 10^{-4}$ mol·dm^{-3}; M/L ratio = 2.1; pH = 5; positive ion mode.

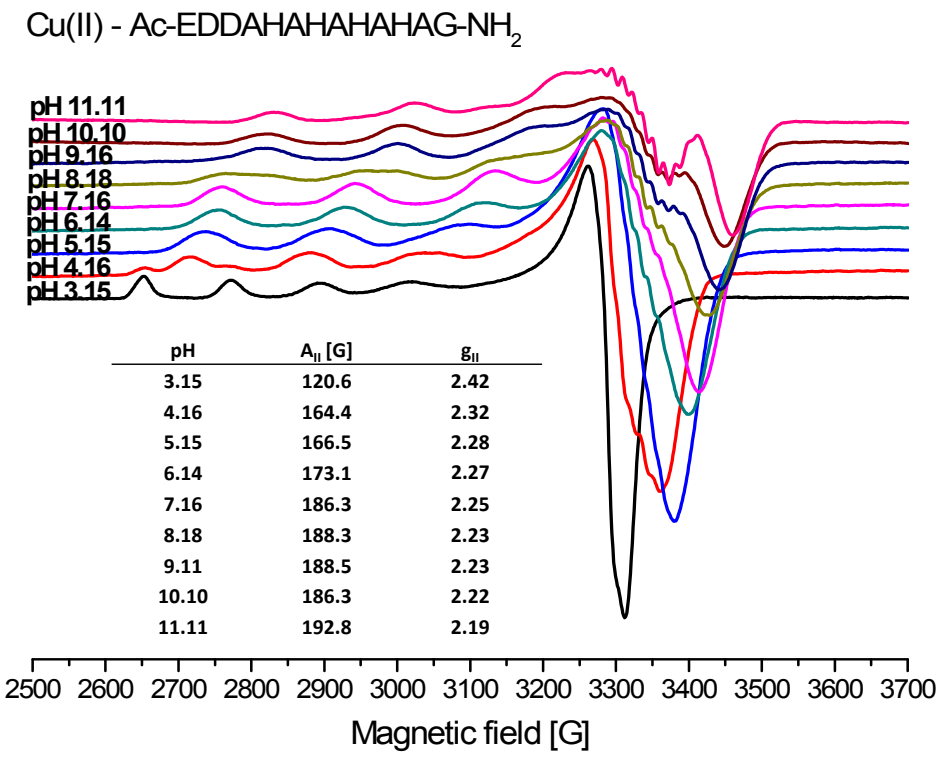

pH	A_{II} [G]	g_{II}
3.15	120.6	2.42
4.16	164.4	2.32
5.15	166.5	2.28
6.14	173.1	2.27
7.16	186.3	2.25
8.18	188.3	2.23
9.11	188.5	2.23
10.10	186.3	2.22
11.11	192.8	2.19

Figure S12. EPR spectra at different pH for the system Cu(II)/L1; $C°_{Cu(II)} = 1 \cdot 10^{-3}$ mol·dm^{-3}; M/L ratio = 1.1.1.

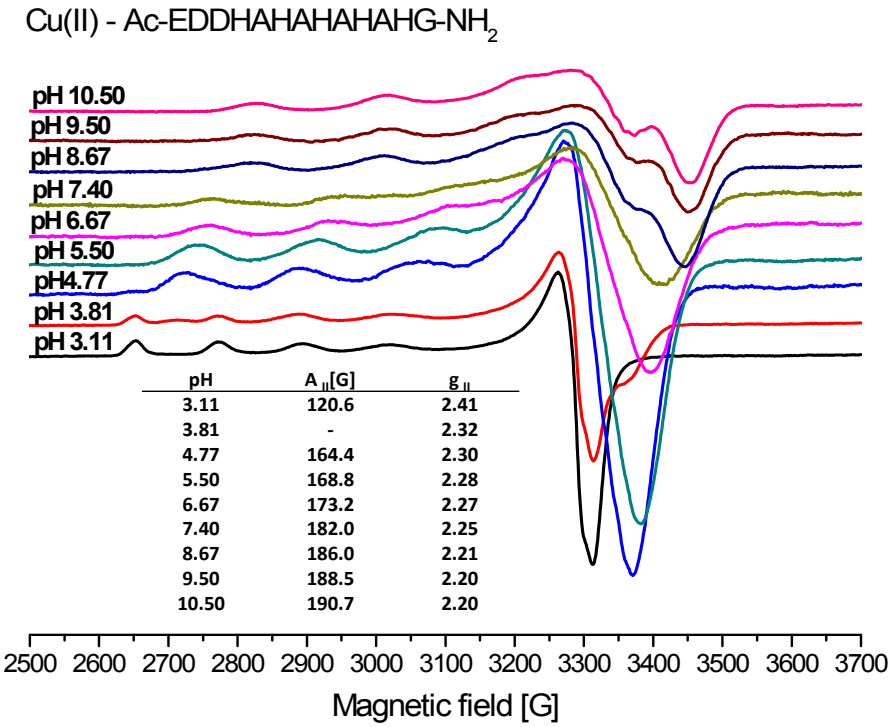

Figure S13. EPR spectra at different pH for the system Cu(II)/L2; $C°_{Cu(II)} = 1 \cdot 10^{-3}$ mol·dm^{-3}; M/L ratio = 1.1.1.

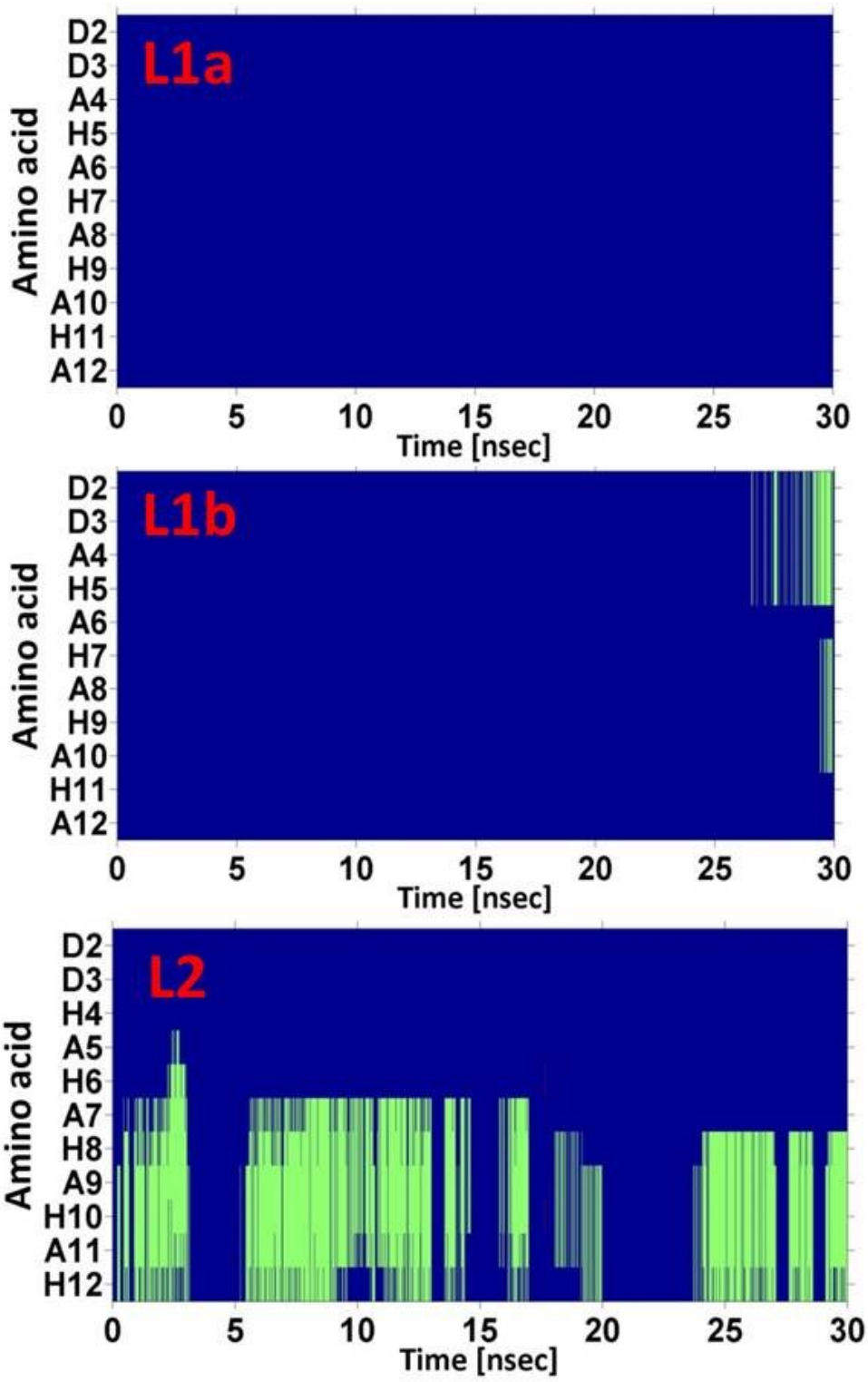

Figure S14 DSSP calculations for each residue along the peptides along the time of the simulations.

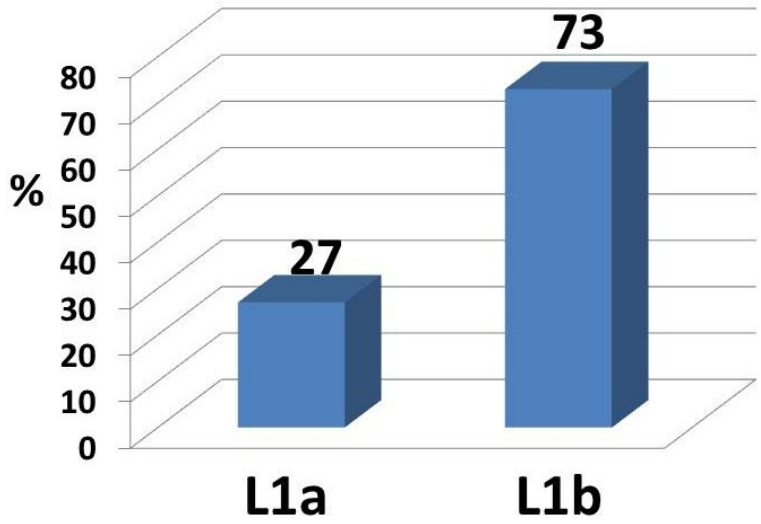

Figure S15 Populations of the simulated peptides L1a and L1b models. The populations had been estimated via Monte Carlo simulations.

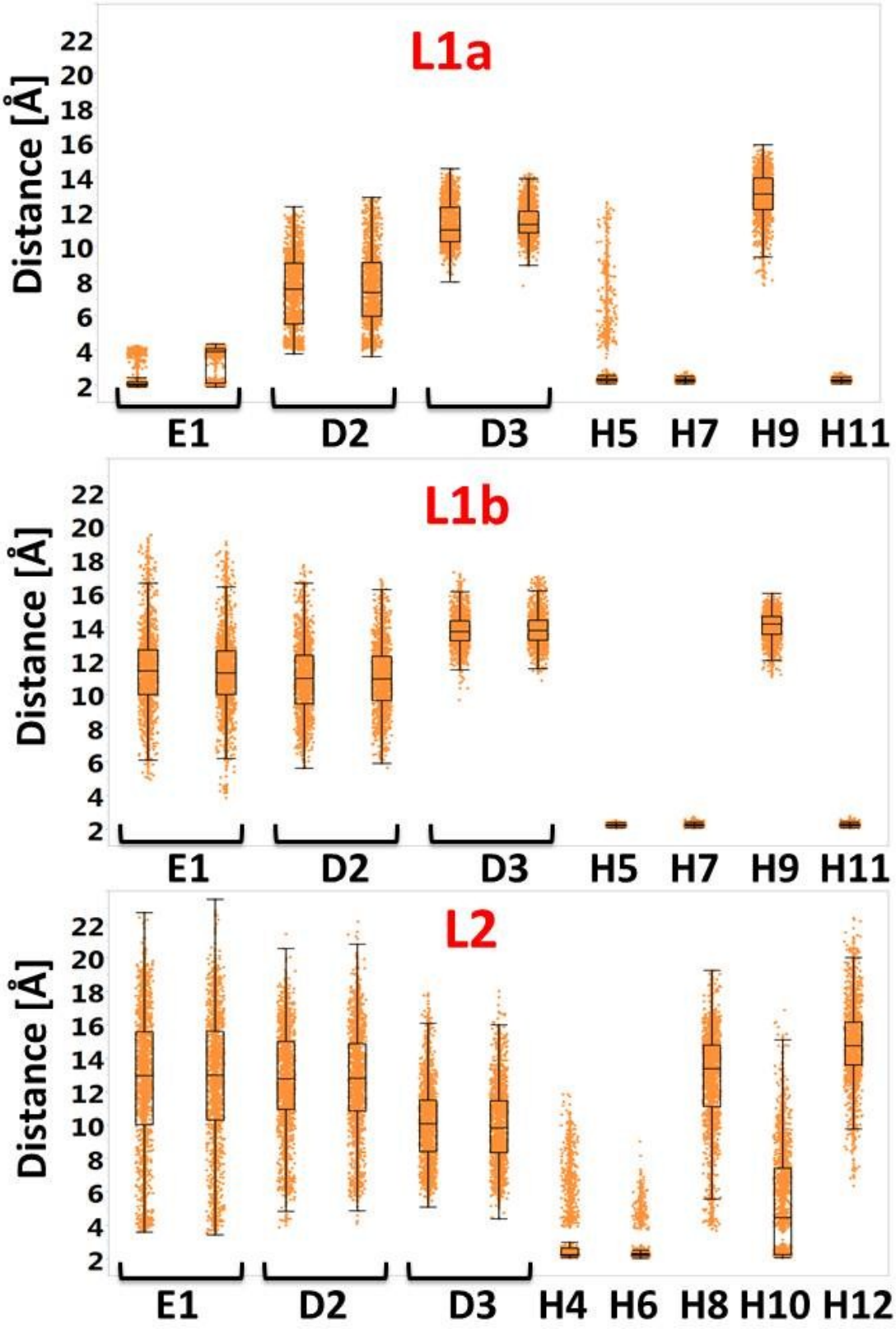

Figure S16 The Cu(II)-Nε (His) atom and Cu(II)-O (carboxyl group) atoms distance distribution for each His residue obtained from MD simulations for the structures L1a, L1b and L2. The vertical lines within each box represent the median distance values.

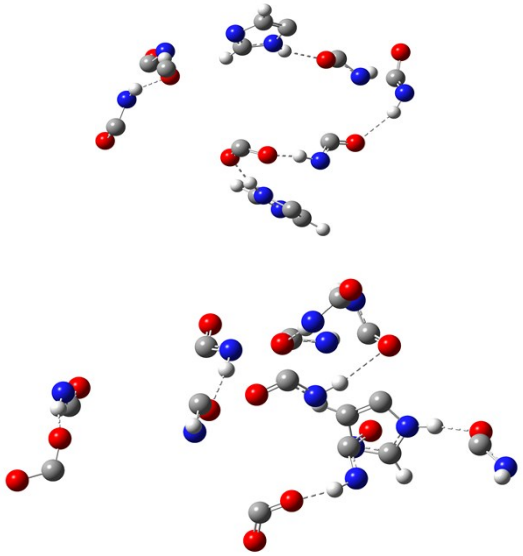

L2

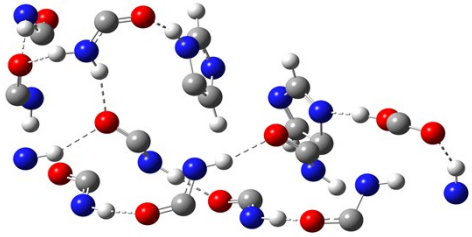

Figure S17. Synthetic network of hydrogen bonds in Complexes L1a, L1b and L2.

(a)

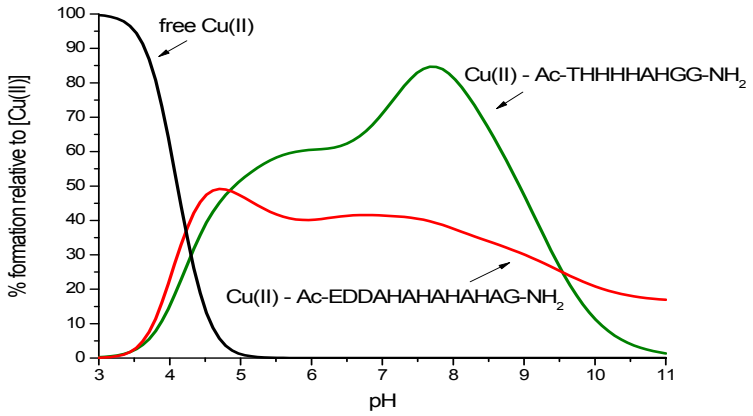

(b)

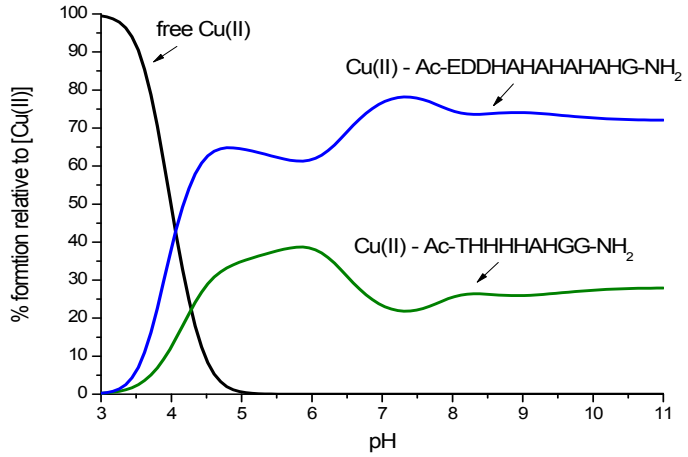

Figure S18. Competition plot for a ternary solution containing equimolar concentrations (1 mM) of: (a) Cu(II), L1 and Ac-THHHHAHGG-NH_2 (*H. pylori*); (b) Cu(II), L2 and Ac- THHHHAHGG-NH_2 (*H. pylori*).

(a)

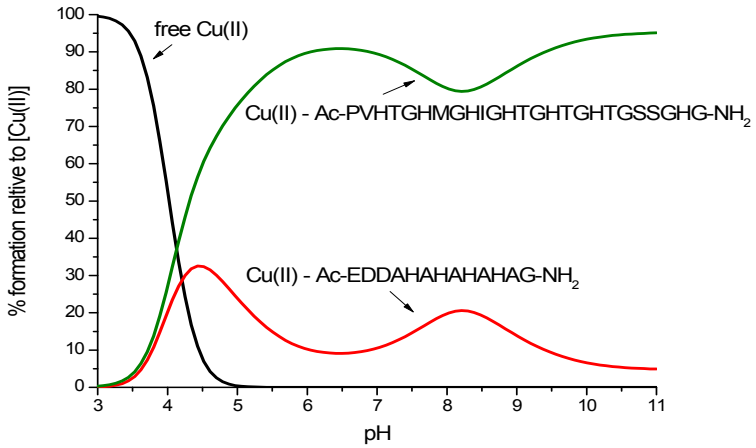

(b)

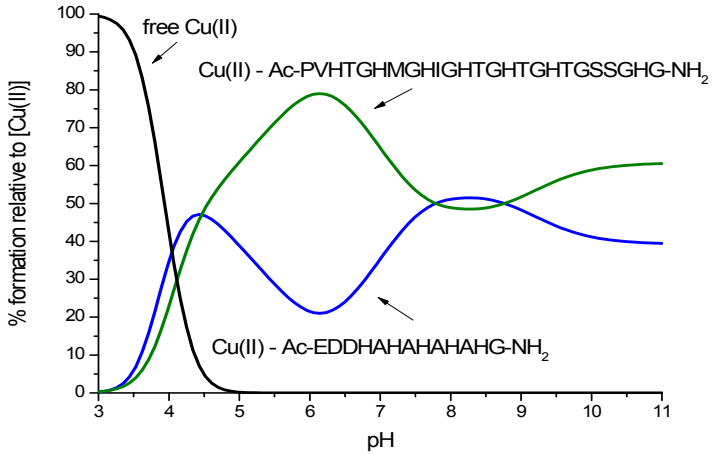

Figure S19. Competition plot for a ternary solution containing equimolar concentrations (1 mM) of: (a) Cu(II), L1 and Ac-PVHTGHMGHIGHTGHTGHTGHTGSSHG-NH_2 (zp-PrP63-87); (b) Cu(II), L2 and Ac- PVHTGHMGHIGHTGHTGHTGHTGSSHG-NH_2 (zp-PrP63-87).

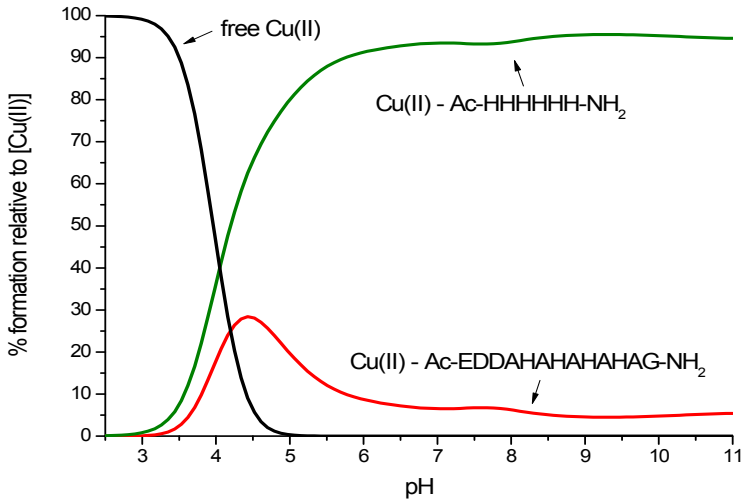

(a)

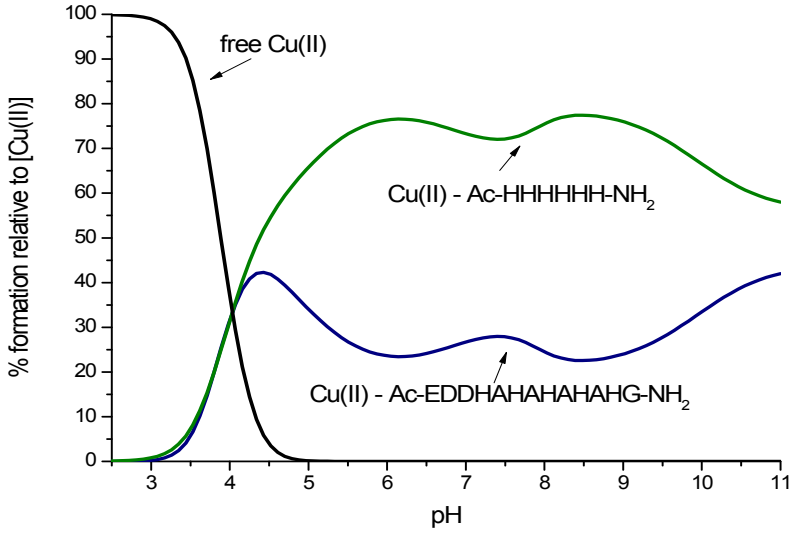

(b)

Figure S20. Competition plot for a ternary solution containing equimolar concentrations (1 mM) of: (a) Cu(II), L1 and Ac-HHHHHH-NH_2 (His_6-tag) ; (b) Cu(II), L2 and Ac-HHHHHH-NH_2 (His_6-tag).